Hong Kong J Radiol. 2021;24:129-40 | https://doi.org/10.12809/hkjr2117210

PICTORIAL ESSAY

Imaging Spectrum of Sellar and Parasellar Masses in a Paediatric Population: a Pictorial Essay

S Gupta, S Singh, R Dixit, A Prakash

Department of Radiology, Maulana Azad Medical College, India

INTRODUCTION

Tumours in the sellar and suprasellar regions are not uncommon in the paediatric population and differ to adult sellar tumours with respect to type and frequency. Such masses comprise about 10% of all paediatric brain tumours.[1] Magnetic resonance imaging (MRI) renders high intrinsic soft tissue contrast and greater anatomic detail. It remains the mainstay in diagnosis and characterisation of these lesions. Computed tomography may provide complimentary information, especially in identifying the presence of calcifications. The first step in diagnosing these lesions is to determine their anatomic location, followed by an assessment of their intrinsic signal and enhancement pattern. Cystic component / calcification also needs to be looked at as it aids characterisation of the lesions (Figure 1). The clinical symptoms and hormonal profile along with the age of the child are also important to narrow down the list of differential diagnoses. Clinical symptoms can be non-specific due to raised intracranial pressure or specifically related to hormonal derangement. Altered vision may occur secondary to mass effect on the optic apparatus.[1,2]

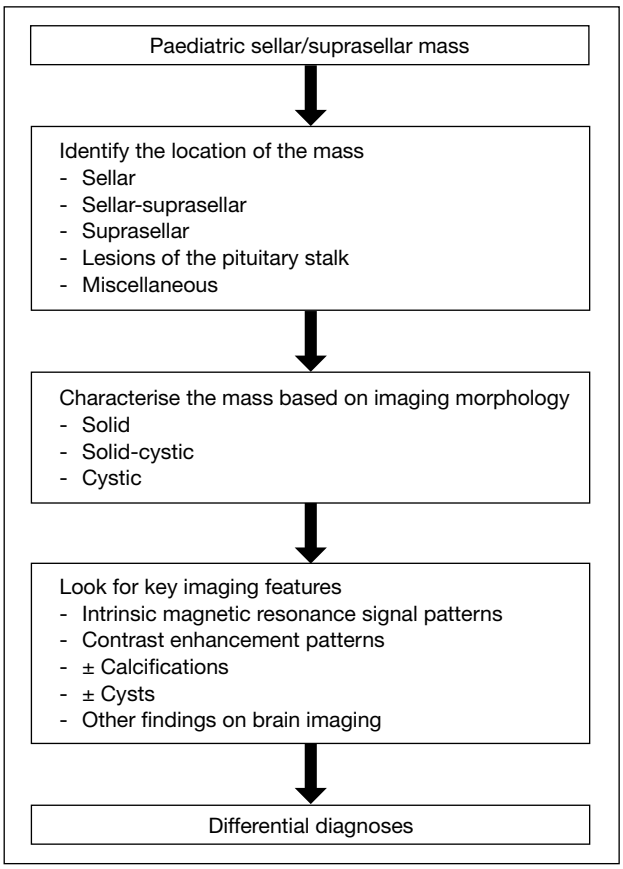

Figure 1. Approach to paediatric sellar/suprasellar/parasellar masses.

NORMAL ANATOMY

The sellar, suprasellar, and parasellar regions are an anatomically complex area (Figure 2). The pituitary

Correspondence: *Dr S Gupta, Department of Radiology, Maulana Azad Medical College, India*
Email: surabhig27@gmail.com

Submitted: 8 Apr 2020; Accepted: 24 Aug 2020

Contributors: All authors designed the study, acquired the data, analysed the data, drafted the manuscript, and critically revised the manuscript for important intellectual content. All authors had full access to the data, contributed to the study, approved the final version for publication, and take responsibility for its accuracy and integrity.

Conflicts of Interest: The authors declare no conflicts of interest.

Funding/Support: This pictorial essay received no specific grant from any funding agency in the public, commercial or not-for-profit sectors.

Ethics Approval: Ethical approval was requested and obtained from the institutional ethics committee. Patient consent was obtained in each case.

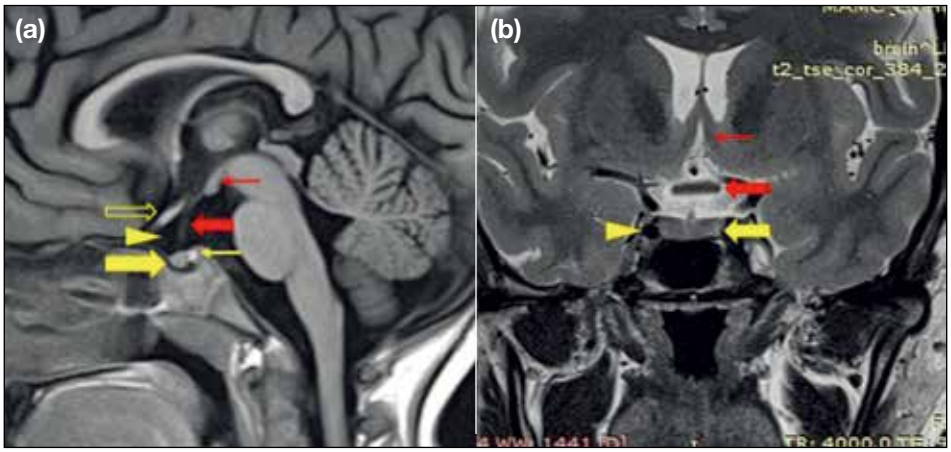

Figure 2. Normal anatomy. (a) Sagittal T1-weighted image, anterior pituitary isointense on T1-weighted (yellow arrow), posterior pituitary bright on T1-weighted (thin yellow arrow), pituitary stalk (red arrow), optic tract (open yellow arrow), suprasellar cistern (yellow arrowhead), and mamillary body (thin red arrow). (b) Coronal T2-weighted image: pituitary gland (yellow arrow), optic chiasma (red arrow), flow void of right internal cerebral artery (yellow arrowhead), and third ventricle (thin red arrow).

fossa is a spherical depression in the sphenoid bone, bounded by the sphenoid sinus antero-inferiorly, the cavernous sinuses laterally, diaphragm sellae and the hypothalamus superiorly, and dorsum sellae and the brainstem posteriorly. The suprasellar cistern is an expansion of the subarachnoid space and contains the optic nerves, chiasma, tracts, Circle of Willis, and pituitary stalk / infundibulum. The hypothalamus forms the floor and lateral walls of the third ventricle. The tuber cinereum is a ridge of tissue between the infundibulum and mammillary bodies. The pituitary gland is composed of two parts: the adenophysis, isointense to brain on both T1-weighted (T1W) and T2-weighted (T2W) images and the neurohypophysis, seen as a bright spot on T1W images. The anterior lobe appears hyperintense like the posterior lobe in newborns and becomes T1 isointense by 6 to 8 weeks of life.[3]

Craniopharyngioma

Craniopharyngiomas are the most common paediatric intracranial tumours of non-glial origin, accounting for up to 10% of paediatric brain tumours[4] and 50% of paediatric suprasellar tumours.[5] Histologically, there are two subtypes: the adamantinomatous type that has a bimodal distribution and is mostly seen in children, and the squamous papillary type that is seen mostly in adults (Table 1). Craniopharyngiomas are most commonly both intrasellar and suprasellar (53-75%), followed by purely suprasellar (20-41%) and, rarely, purely intrasellar.[6] Computed tomography scan is useful for detecting calcifications that may present in up to 87% of the cases (Figure 3).

Adamantinomatous craniopharyngiomas on MRI (Figure 4) appear as lobulated solid-cystic masses in the suprasellar and/or sellar region. Solid components are isointense on T1W and hyperintense on T2W images and show enhancement. The cyst contents can be T1 hyperintense in about 33% cases due to high proteinaceous / cholesterol / haemorrhagic content, referred to as 'Motor-oil' appearance[7] (Figure 4a).

Table 1. Adamantinomatous versus papillary craniopharyngioma.

	Adamantinomatous	Papillary
Age	Bimodal, children (50-60 years)	Adults
Tissue structure	Mostly cystic	Predominantly solid
Fluid	Oil	Fluid
T1-weighted	Hyperintense	Hypointense
Shape	Lobulated	Spherical
Adhesion and infiltration	Yes, to hypothalamus	No
Enhancement	Avid of the solid component	Mild
Calcification	Common (90%)	Rare

Germ Cell Tumours

Germ cell tumours are classified as germinomatous germ cell tumours or non-germinomatous GCTs. They usually arise in the pineal region, followed by the suprasellar cistern. Smaller lesions tend to be homogenous and are centred in the pituitary stalk. Thickening of the pituitary stalk with absence of the normal T1 hyperintense neurohypophysis bright spot may be seen. Larger lesions tend to be solid-cystic in appearance (Figure 5), with the solid component usually being isointense to hypointense on T2W imaging. The lesions show heterogenous post-contrast enhancement (Figure 6a). The risk of leptomeningeal dissemination emphasises the importance of imaging the entire craniospinal axis[8] (Figure 6b).

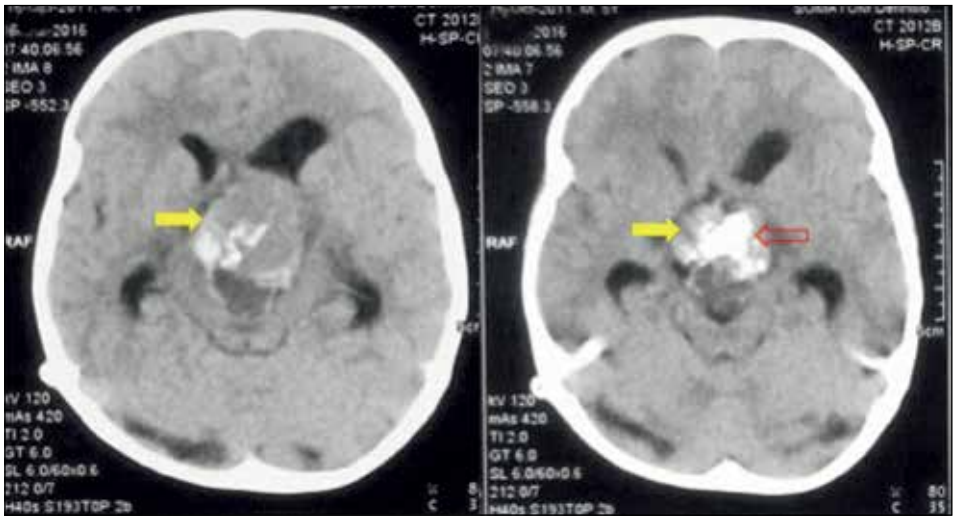

Figure 3. Craniopharyngioma. Axial computed tomography images showing hyperdense mass (yellow arrows) in sellar-suprasellar region with calcification (red open arrow) within.

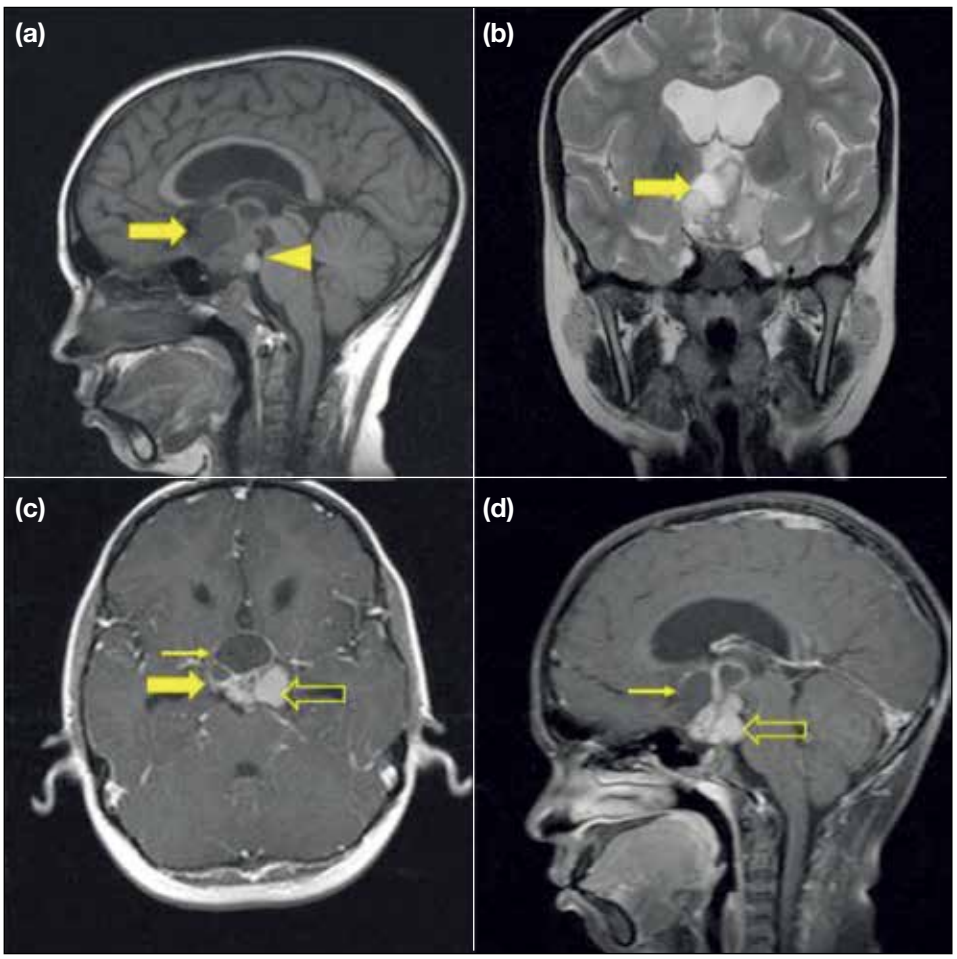

Figure 4. Adamantinomatous craniopharyngioma. (a) Sagittal T1-weighted, (b) coronal T2-weighted, and contrast-enhanced (c) axial and (d) sagittal magnetic resonance images showing a solid cystic mass (arrows) in the sellar-suprasellar region, appearing hypointense on T1-weighted images with hyperintense focus (arrowhead) suggestive of motor oil appearance, hyperintense on T2-weighted images showing homogenous contrast enhancement of solid component (open arrows) and peripheral enhancement of the cystic component (thin arrow).

Synchronous involvement of the pineal and suprasellar regions may be evident in up to 15% of cases and are termed bifocal germinomas[9] (Figure 7). Cases of occult germinomas show only the absence of a posterior pituitary bright spot on MRI with an infundibular mass seen on follow-up scans after 14 months[10] (Figure 8).

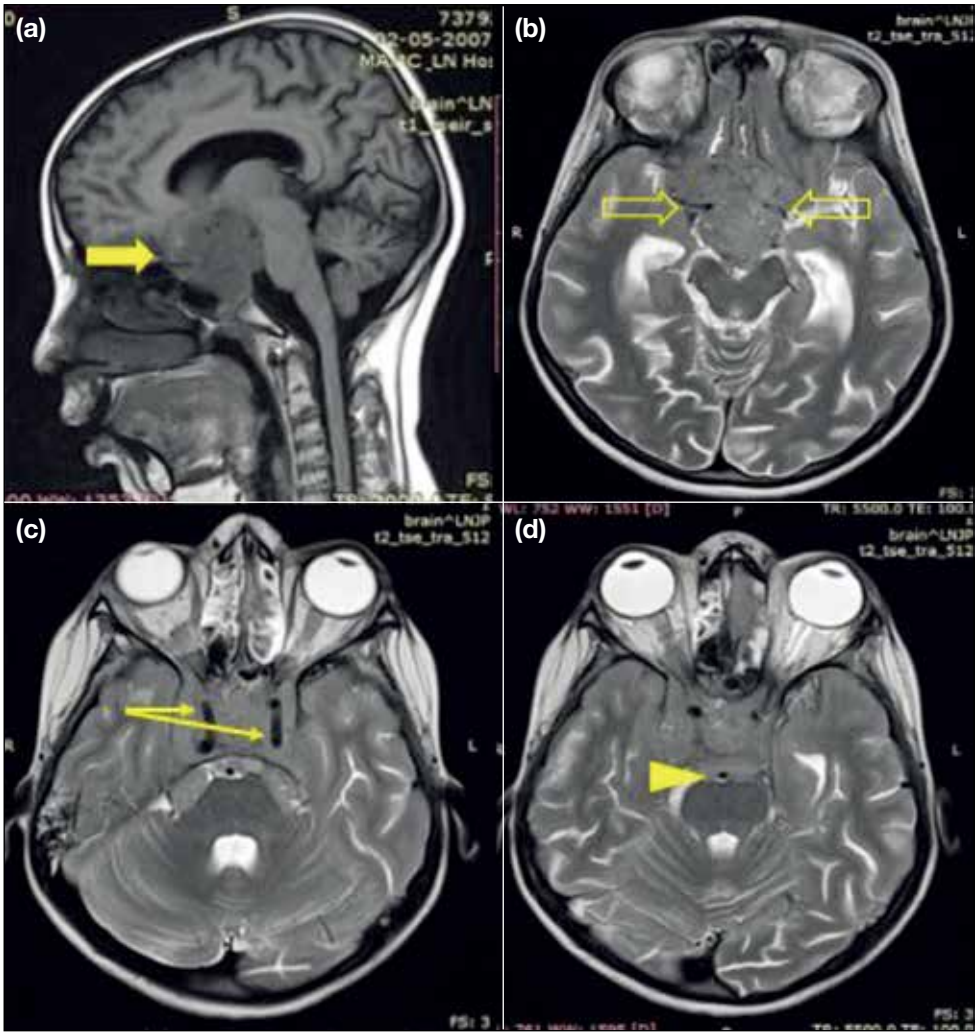

Figure 5. Germ cell tumours. (a) Sagittal T1-weighted and (b to d) axial T2-weighted magnetic resonance imaging images showing a solid lesion (arrow) in the sella-suprasellar region appearing hypointense on T1-weighted images and isointense on T2-weighted images. Encasement of bilateral proximal middle cerebral arteries (open arrows), bilateral internal carotid arteries (thin arrows), and posterior encasement of the basilar artery (arrowhead) are evident.

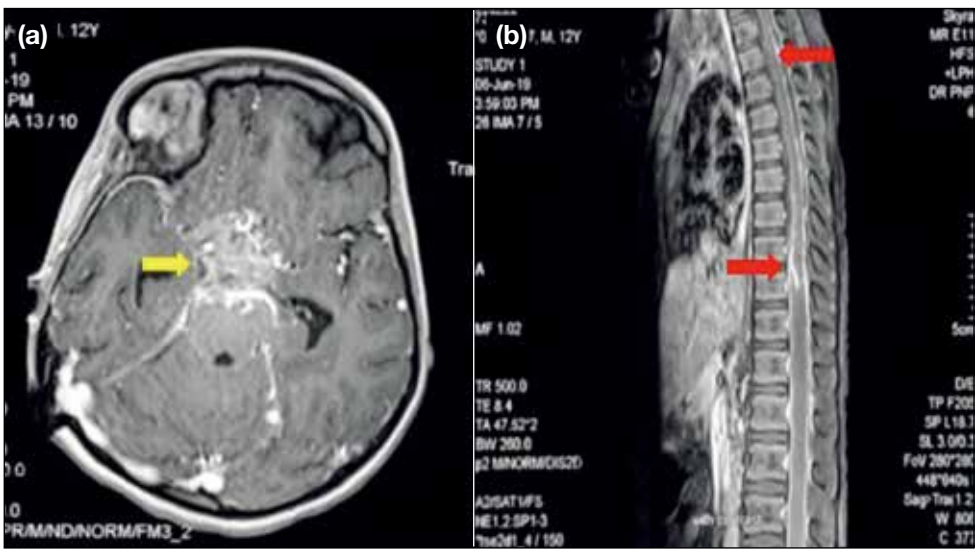

Figure 6. In the same case, T1-weighted post-contrast (a) axial and (b) sagittal spine magnetic resonance images show intense enhancement of the mass (yellow arrow) with intense leptomeningeal enhancement along the spinal cord (red arrows), indicating metastasis.

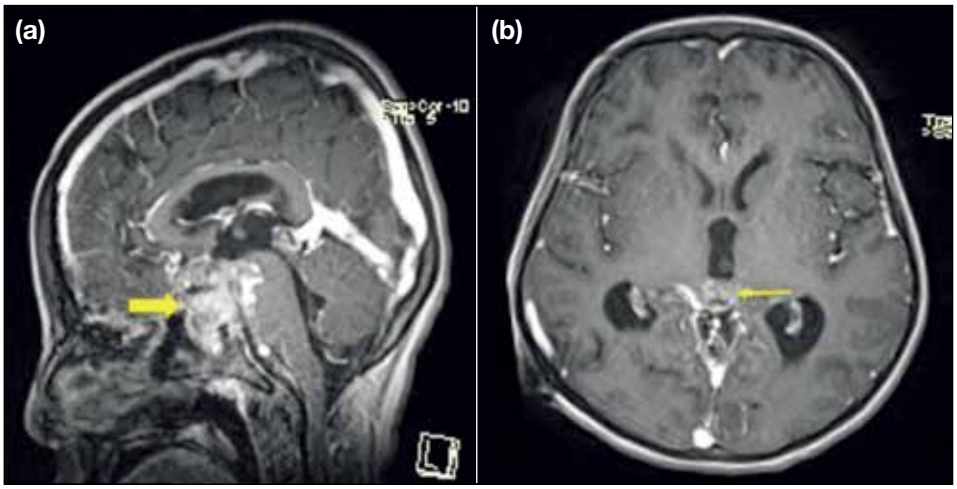

Figure 7. Bifocal germinoma. (a) Sagittal and (b) axial post-contrast brain magnetic resonance imaging images showing a solid enhancing lesion (arrow) in the sellar-suprasellar region with a similar enhancing lesion in the pineal region (thin arrow).

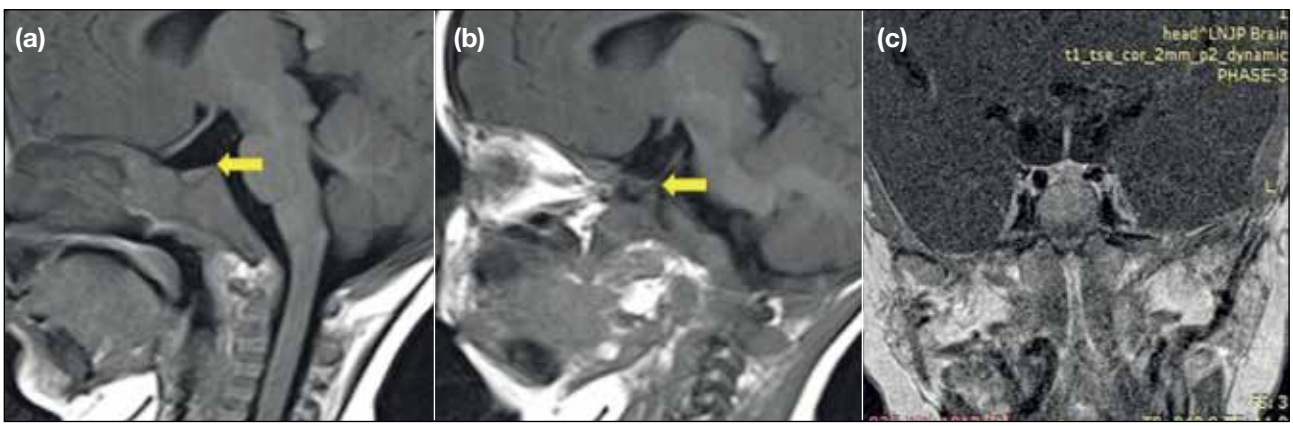

Figure 8. Occult germinoma. (a, b) Sagittal T1-weighted and (c) coronal post-contrast T1-weighted brain magnetic resonance images showing absence of the normal pituitary bright spot (arrows) with no lesion in the pituitary gland.

Hypothalamic Chiasmatic Glioma

Hypothalamic chiasmatic glioma (HCGs) are mostly low-grade World Health Organization grade I astrocytomas and invade the brain along the optic pathways. Around 20% to 50% of the HCGs are associated with neurofibromatosis type 1 (NF1).[5] In patients with NF1, the optic nerve is usually affected, resulting in fusiform expansion and kinking. Sporadic non-NF1-associated hypothalamic-chiasmatic gliomas show chiasmatic involvement more commonly with posterior extension beyond the optic pathways.[8] On MRI (Figure 9), HCGs appear as lobulated suprasellar masses, hypo- to iso-intense to grey matter on T1W and hyperintense on T2W images. Intense enhancement is seen following intravenous contrast administration in sporadic HCGs while enhancement is variable in HCGs associated with NF1.[11] Distinguishing hypothalamic gliomas from optic chiasm gliomas can be challenging and is typically determined by locating the epicentre of the lesion and determining optic nerve involvement.

Sellar and Suprasellar Tuberculosis

Sellar tuberculosis represents granulomatous hypophysitis associated with tuberculosis infection. Involvement of the pituitary stalk and sella may be evidenced by thickened, nodular, enhancing stalk and multiple T2 hypointense, peripherally enhancing conglomerate tuberculomas in the sellar and suprasellar region (Figure 10). The presence of parenchymal tuberculomas, nodular leptomeningeal enhancement in basal cisterns and perivascular spaces, help suggest the appropriate diagnosis.[1]

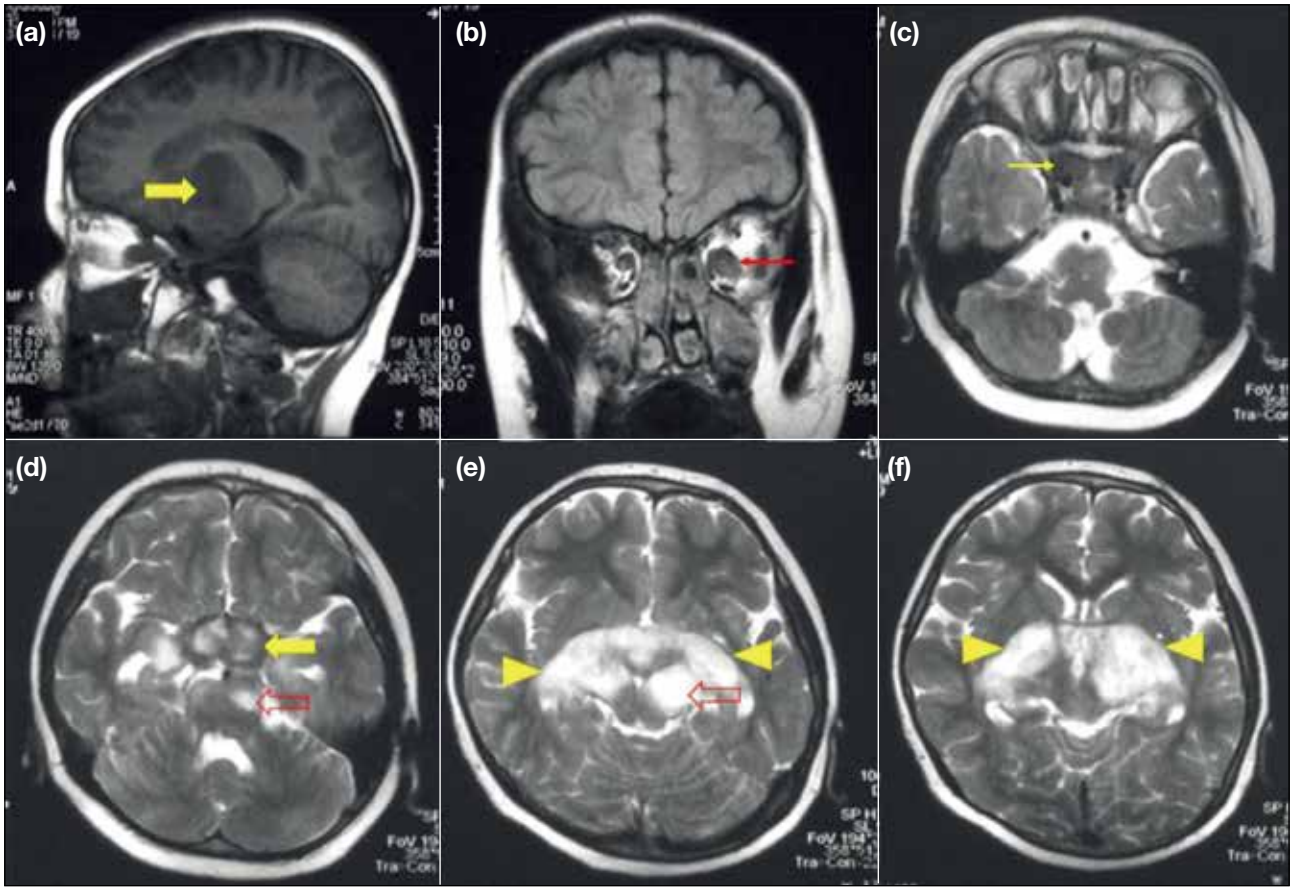

Figure 9. Hypothalamic chiasmatic glioma. Case of neurofibromatosis type 1 (a) sagittal T1-weighted, (b) coronal fluid attenuation inversion recovery, and (c to f) axial T2-weighted brain magnetic resonance images showing dilatation and tortuosity of the left optic nerve (thin red arrow) with involvement of the right optic nerve in the pre-chiasmatic portion (thin yellow arrow) and extension into the optic chiasma (yellow arrows) and retrochiasmatic optic tracts (yellow arrowheads). Areas of T2-weighted hyperintensity seen in the brainstem (red open arrows) represent hamartomatous changes.

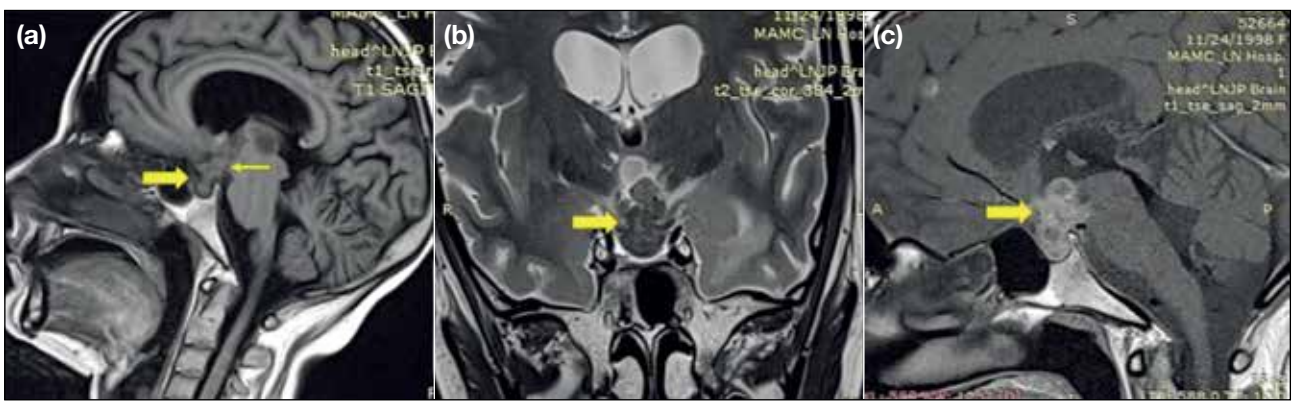

Figure 10. Conglomerate tuberculomas. (a) Sagittal T1-weighted, (b) coronal T2-weighted, and (c) contrast-enhanced sagittal magnetic resonance images showing a solid lesion (arrows) in the sellar-suprasellar region appearing isointense on T1-weighted images, hypointense on T2-weighted images, and showing rim enhancement on post-contrast images. The lesion shows associated infundibular thickening (thin arrow).

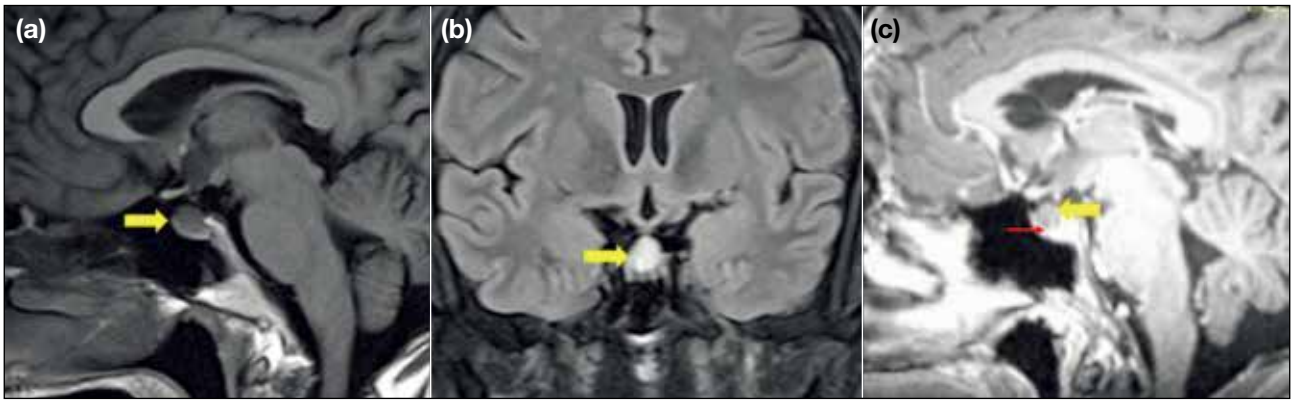

Figure 11. Rathke cleft cysts. (a) Sagittal T1-weighted, (b) coronal fluid attenuation inversion recovery (FLAIR), and (c) contrast-enhanced sagittal magnetic resonance images show a small cystic lesion (yellow arrows) in the sellar region appearing hypointense on T1-weighted images, hyperintense on FLAIR images, and showing no enhancement on post-contrast images. A thin rim of compressed pituitary tissue is seen in the periphery (thin red arrow) of the lesion.

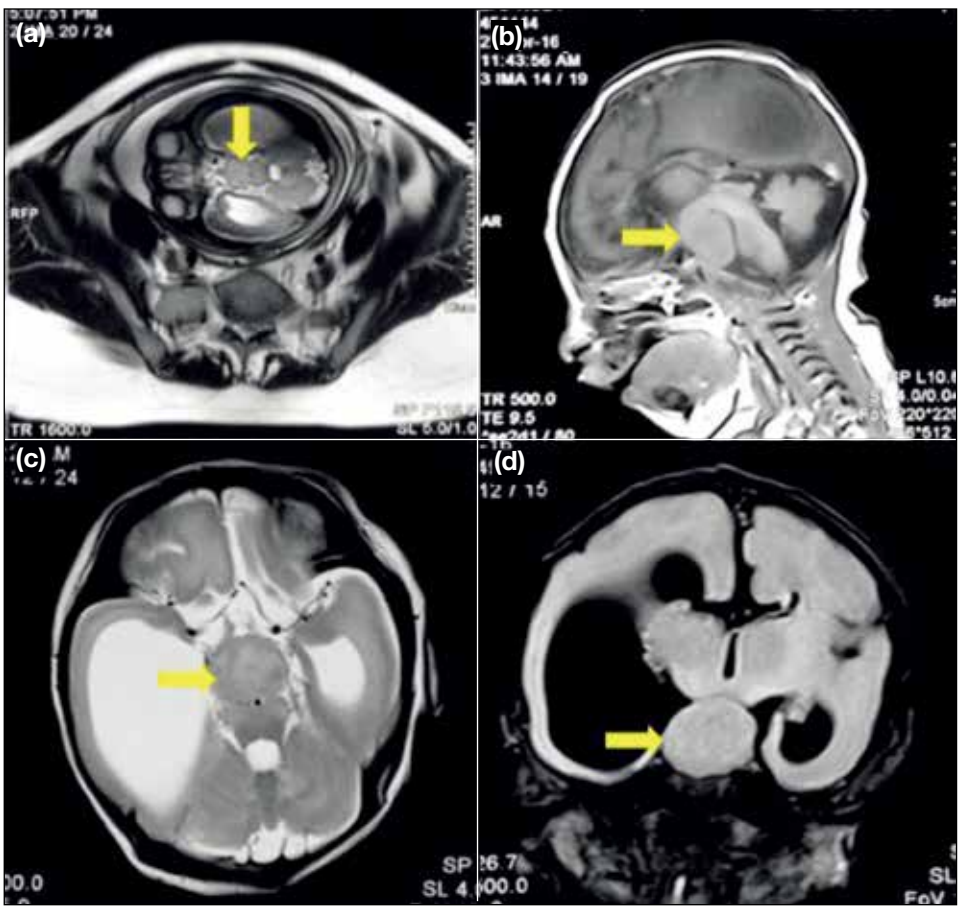

Figure 12. Tuber cinereum hamartoma. (a) Axial T2-weighted fetal, (b) sagittal T1-weighted, (c) axial T2-weighted, and (d) coronal fluid attenuation inversion recovery brain magnetic resonance images in the postnatal period showing a solid lesion (arrows) involving the tuber cinereum appearing isointense to grey matter on all sequences.

Rathke Cleft Cyst

Rathke cleft cyst (RCC) is a cystic remnant of the Rathke pouch that has failed to involute during development. They are less common and smaller in size in children. On imaging, Rathke cleft cysts (Figure 11) can be entirely intrasellar; intrasellar with suprasellar extension; or uncommonly entirely suprasellar. The T1 signal varies depending on the content of the cyst, being hypointense

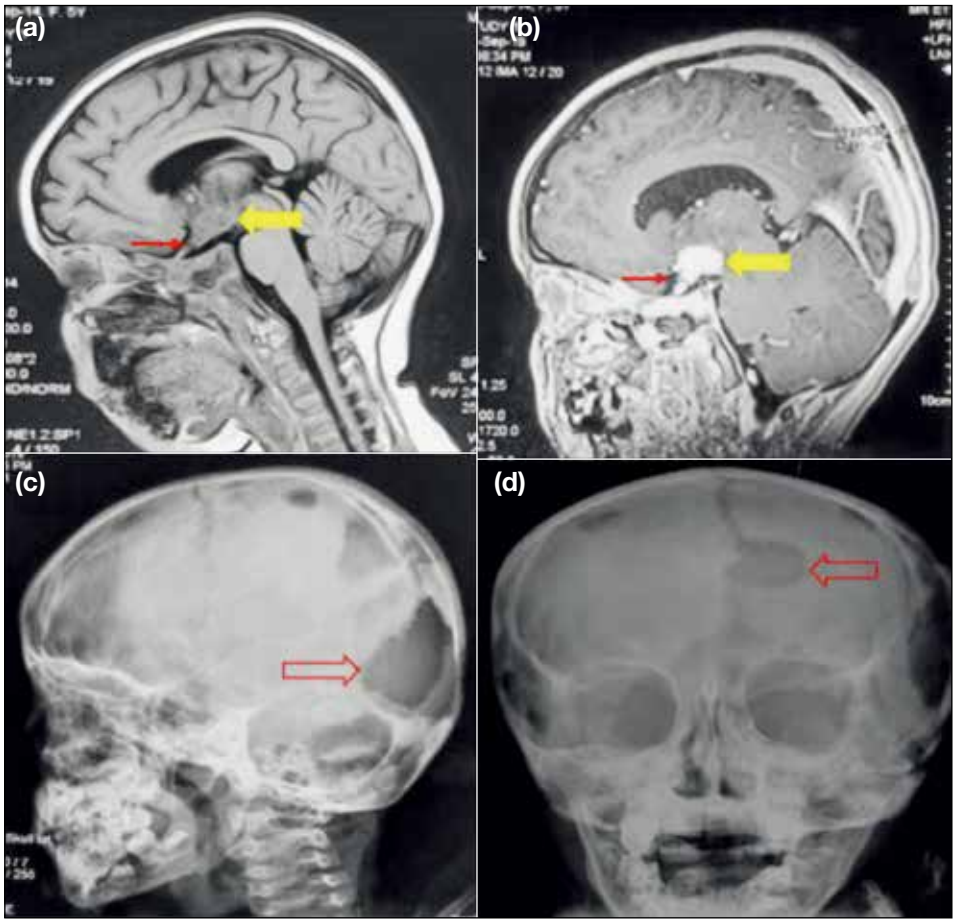

Figure 13. Langerhans cell histiocytosis. (a) Sagittal T1-weighted and (b) post-contrast T1-weighted brain magnetic resonance images showing a solid lesion (yellow arrows) in the suprasellar region appearing hypointense on T1-weighted images with avid homogenous enhancement on post-contrast sequences with thickening of the pituitary stalk (thin red arrows). (c) Lateral and (d) posteroanterior skull radiographs show multiple "punched out" lytic bony lesions (red open arrows) in the calvaria.

with serous cystic contents and hyperintense with proteinaceous / mucoid content. The cyst walls usually do not enhance, but pseudo-enhancement of the walls can be seen if the pituitary gland is compressed along the cyst wall.

Tuber Cinereum Hamartoma

Tuber cinereum hamartomas are congenital grey matter heterotopias in the hypothalamic region and can be detected on antenatal ultrasound. These masses follow grey matter signal on all sequences and do not enhance (Figure 12). The clinical presentation varies with the anatomical location of the lesion. Hamartomas that arise from the floor of the third ventricle project into the interpeduncular cistern and present with precocious puberty. Sessile hamartomas arise from the walls of lower third ventricles. Patients present with gelastic seizures and precocious puberty.[12]

Langerhans Cell Histiocytosis

Langerhans cell histiocytosis (LCH) is an idiopathic disorder that involves the central nervous system in 4% of the paediatric cases. In multicentric LCH, the hypothalamus and pituitary infundibulum are infiltrated in up to 20% of cases.[13] These cases show focal or diffuse thickening of the infundibulum and absence of posterior pituitary bright spot (Figure 13a and b). There is significant overlap of imaging findings between germinomas and LCH. However, calvarial involvement with lytic punched-out bone lesions in the skull (Figure 13c and d) is a finding typically encountered in LCH.

Dermoid and Epidermoid Cysts

These are congenital inclusion cysts. Dermoid cysts are midline extra-axial lesions. They contain variable amounts of dermal derivatives. MRI features depend on the content of the cyst. They are well-defined spherical or lobulated lesions that appear hyperintense on T1W (when fat is present) [Figure 14a] and show heterogenous signal intensity on T2W images. These lesions do not enhance (Figure 14b). Fat-saturated

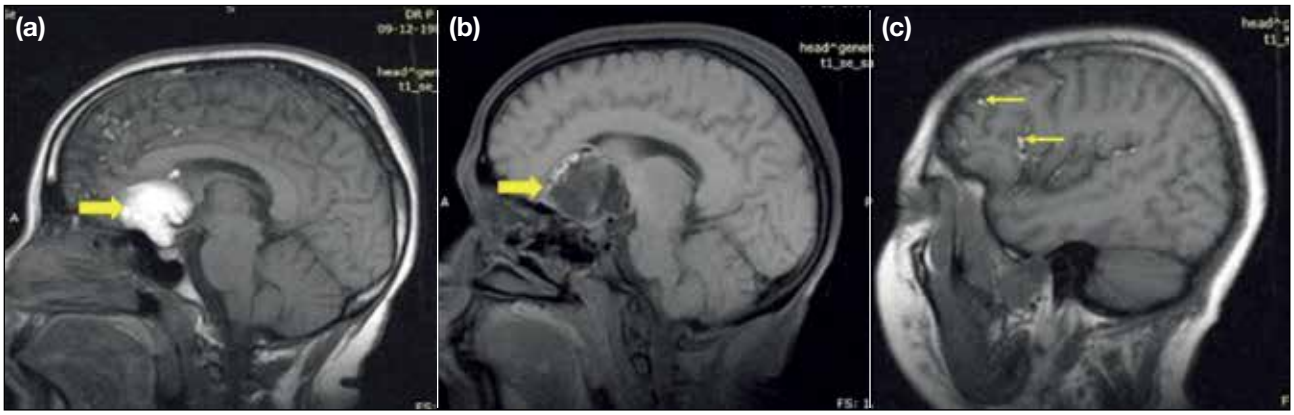

Figure 14. Ruptured dermoid cyst. (a, c) Sagittal T1-weighted and (b) fat-suppressed T1-weighted brain magnetic resonance images showing a suprasellar mass lesion (arrow) appearing hyperintense on T1-weighted images, with complete signal suppression on fat-suppressed images (arrow). Few fat signal droplets (thin arrows) are seen in the subarachnoid space, suggestive of ruptured dermoid cyst.

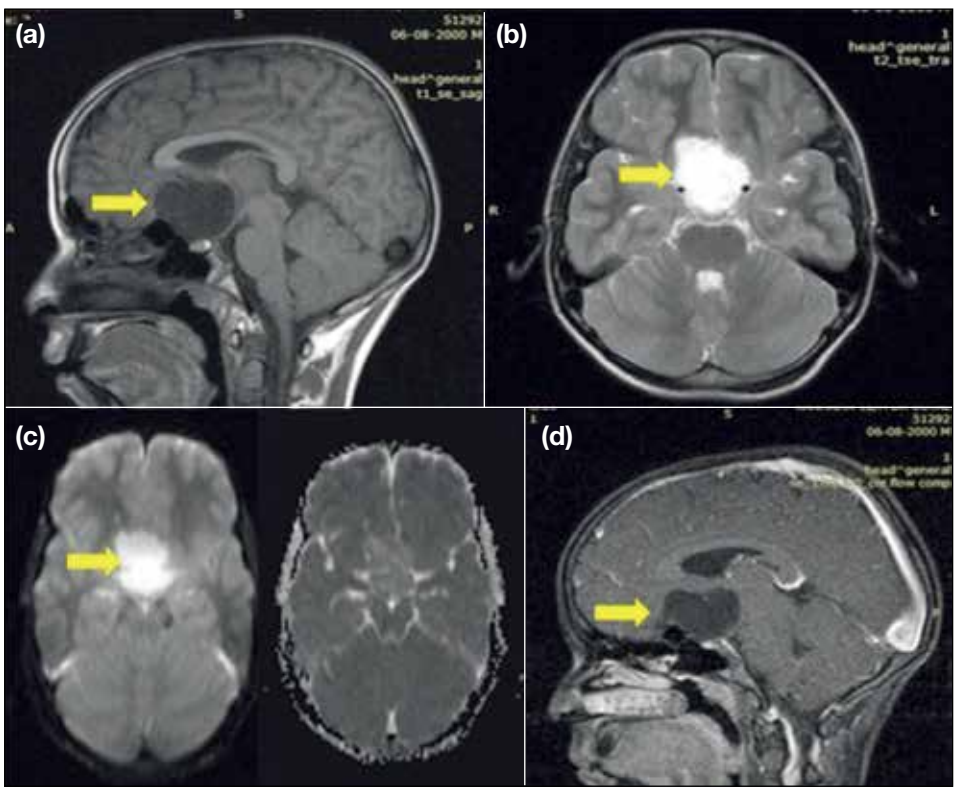

Figure 15. Epidermoid cyst. (a) Sagittal T1-weighted, (b) axial T2-weighted, (c) diffusion-weighted imaging with apparent diffusion coefficient (DWI-ADC), and (d) sagittal T1-weighted post-contrast brain magnetic resonance images showing a solid lesion (arrows) in the suprasellar region appearing hypointense on T1-weighted images, hyperintense on T2-weighted images, with restricted diffusion on DWI-ADC images, and no significant enhancement on T1-weighted post-contrast sequences.

images can be acquired to show signal dropout of fatty component. Numerous T1 hyperintense foci are seen involving in the subarachnoid spaces in cases of ruptured dermoid cysts (Figure 14c).

Epidermoid cysts are off-midline extra-axial lesions. The epidermoids with low protein content follow the cerebrospinal fluid (CSF) signal intensity on conventional sequences with partial suppression on fluid attenuation inversion recovery sequences and no contrast enhancement (Figure 15a, b and d). However, the definitive diagnosis can be suggested by diffusion weighted imaging, where epidermoids show true diffusion restriction (Figure 15c).

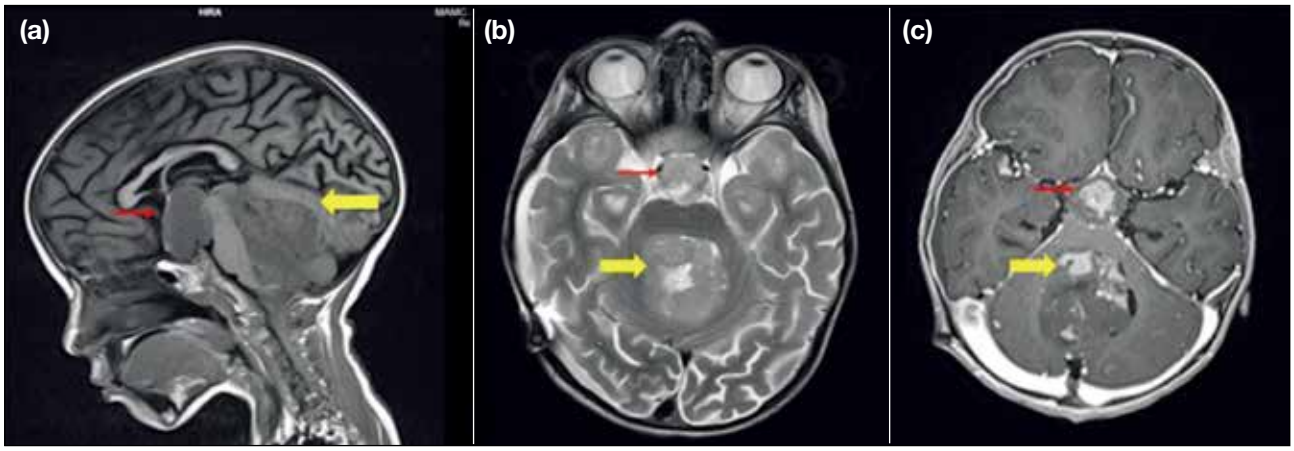

Figure 16. Suprasellar metastases from medulloblastoma. (a) Sagittal T1-weighted, (b) axial T2-weighted, and (c) post-contrast T1-weighted brain magnetic resonance images showing a solid mass in the posterior fossa (yellow arrows) and sellar-suprasellar region (thin red arrows), appearing hypointense on T1-weighted and T2-weighted images with heterogenous post-contrast enhancement on T1-weighted post-contrast sequences.

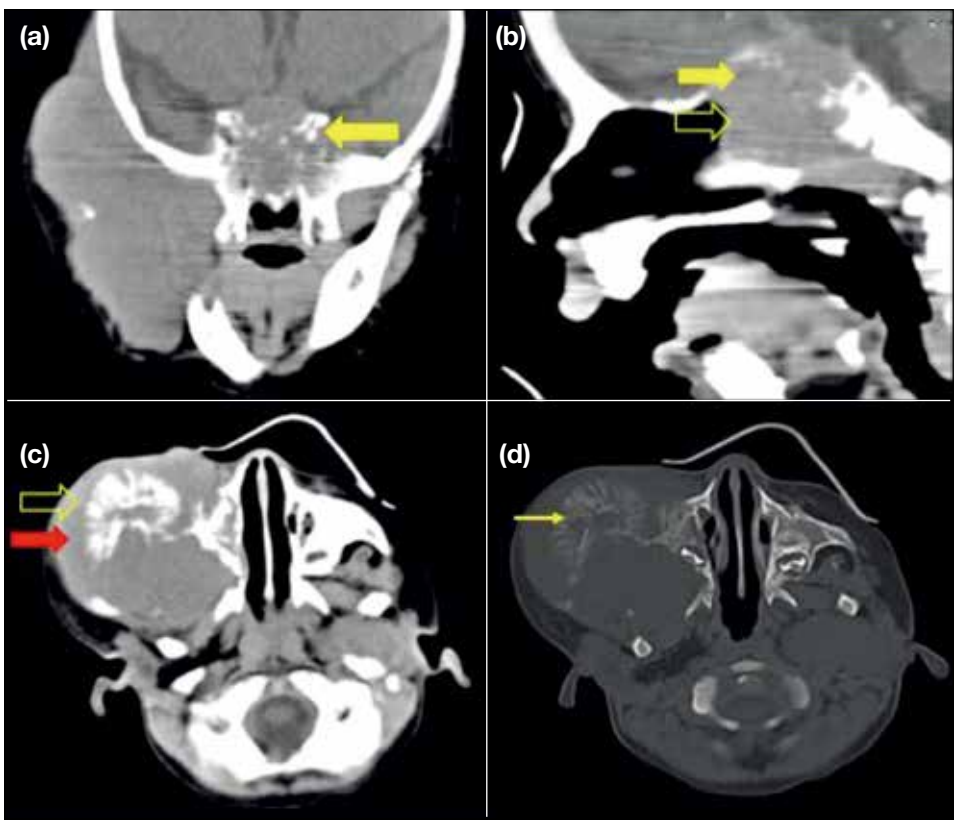

Figure 17. Sellar/suprasellar metastases from neuroblastoma. (a) Coronal and (b) sagittal non-contrast soft tissue window, (c) axial soft tissue, and (d) bone window brain and face computed tomography images showing solid mass lesions in the sellar-suprasellar (yellow arrows) and right infratemporal (red arrow) regions with large extraosseous soft tissue (open yellow arrows) and bony destruction having a spiculated sunburst appearance (thin yellow arrow).

Metastasis

Metastasis to the sellar and suprasellar region can disseminate through both CSF seeding and via a haematogenous route. The most favoured site for metastatic deposits via CSF spread is the infundibular recess. The posterior pituitary gland and the pituitary stalk are common sites of involvement in haematogenous metastasis. Intracranial tumours with a high predilection for CSF dissemination include medulloblastoma, ependymoma, germinoma,

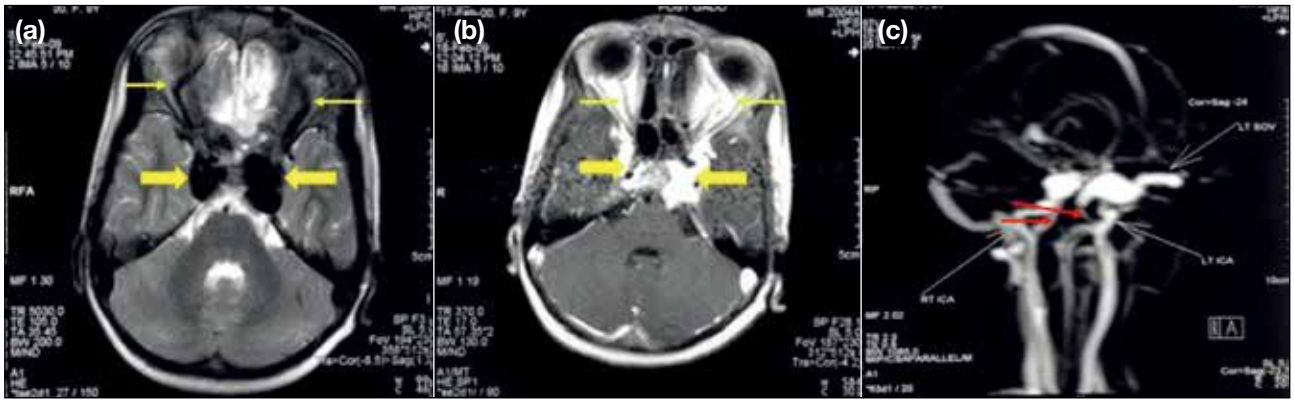

Figure 18. Bilateral carotid-cavernous fistulae. (a) Axial T2-weighted and (b) post-contrast T1-weighted brain magnetic resonance images showing dilated and tortuous cavernous sinuses (yellow arrows) with dilated superior ophthalmic veins (thin yellow arrows) seen as flow voids on T2-weighted images with intense enhancement on post-contrast images. (c) Maximum intensity projection magnetic resonance angiogram showing communication (thin red arrows) of the intracavernous segments of the internal carotid artery with the cavernous sinus with retrograde filling of the superior ophthalmic veins.

pineoblastoma, neuroblastoma of the skull base and lymphomatous tumours. The MRI features of metastatic disease depend on the underlying primary tumour and include focal sellar/parasellar lesions with/without leptomeningeal enhancement[14] (Figures 16 and 17).

Vascular Malformations

Many vascular anomalies may involve the parasellar region, including cavernous malformations, carotid-cavernous fistulas, arterial aneurysms of the ophthalmic artery, arteriovenous malformations, and venous malformations. Cavernous malformations are the most common. Vascular malformations are commonly seen as T2 hyperintense lesions with hypointense rim representing haemosiderin; however, high-flow vascular malformations may show flow voids and appear T2 hypointense. Carotid-cavernous fistulas are best demonstrated on MR angiography that shows the fistulous communication (Figure 18).

CONCLUSION

Sellar and parasellar masses are not uncommon in the paediatric age-group. Their type and frequency differ to those encountered in adults. Craniopharyngiomas represent almost half of sellar region tumours in children, followed by hypothalamic-chiasmatic gliomas, hypothalamic hamartomas and germinomas. Assessment of the site of origin, signal characteristics and enhancement patterns along with clinical presentation and age of the child can help narrow the differentials and reach a definitive diagnosis (Table 2).

REFERENCES

1. Seeburg DP, Dremmen MH, Huisman TA. Imaging of the sella and parasellar region in the pediatric population. Neuroimaging Clin N Am. 2017;27:99-121.
2. Taylor M, Couto-Silva AC, Adan L, Trivin C, Sainte-Rose C, Zerah M, et al. Hypothalamic-pituitary lesions in pediatric patients: endocrine symptoms often precede neuro-ophthalmic presenting symptoms. J Pediatr. 2012;161:855-63.
3. Kitamura E, Miki Y, Kawai M, Itoh H, Yura S, Mori N, et al. T1 signal intensity and height of the anterior pituitary in neonates: correlation with postnatal time. AJNR Am J Neuroradiol. 2008;29:1257-60.
4. Bourekas EC, Miller JW, Christoforidis GA. Masses of the sellar and juxtasellar region. In: Drevelegas A, editor. Imaging of Brain Tumors with Histological Correlations. Heidelberg (Berlin): Springer; 2002. p 227-52.
5. Plaza MJ, Borja MJ, Altman N, Saigal G. Conventional and advanced MRI features of pediatric intracranial tumors: posterior fossa and suprasellar tumors. AJR Am J Roentgenol. 2013;200:1115-24.
6. Karavitaki N, Wass JA. Craniopharyngiomas. Endocrinol Metab Clin North Am. 2008;37:173-93.
7. Kumar J, Kumar A, Sharma R, Vashisht S. Magnetic resonance imaging of sellar and suprasellar pathology: a pictorial review. Curr Probl Diagn Radiol. 2007;36:227-36.
8. Derman A, Shields M, Davis A, Knopp E, Fatterpekar GM. Diseases of the sella and parasellar region: an overview. Semin Roentgenol. 2013;48:35-51.
9. Echevarría ME, Fangusaro J, Goldman S. Pediatric central nervous system germ cell tumors: a review. Oncologist. 2008;13:690-9.
10. Mootha SL, Barkovich AJ, Grumbach MM, Edwards MS, Gitelman SE, Kaplan SL, et al. Idiopathic hypothalamic diabetes insipidus, pituitary stalk thickening, and the occult intracranial germinoma in children and adolescents. J Clin Endocrinol Metab. 1997;82:1362-7.
11. Vinhais S, Nunes S, Salgado D. Optic gliomas in children — a review on MR imaging findings. Annual Meeting of the European Congress of Radiology; 2015 March 4-8; Vienna, Austria. Poster

Table 2. Clinical and neuroimaging features of paediatric sellar-suprasellar masses and parasellar masses.

Lesion	Demographics	Clinical features	Distinguishing imaging features
Craniopharyngiomas	Common between age 8 and 12 years	Headache, visual disturbance, endocrine abnormalities	Commonly suprasellar with intrasellar extension, lobulated solid-cystic tumours with calcifications (better seen on CT). Occasionally T1 hyperintense contents give rise to 'motor oil appearance'
Germ cell tumours	Peak incidence between age 10 and 14 years	Visual disturbances caused by chiasm compression and diabetes insipidus caused by pituitary axis dysfunction CSF and blood may show β-human chorionic gonadotropin or α-fetoprotein	Hypo- or iso-intense on T1W and hyperintense on T2W images, with intense contrast enhancement with thickening of pituitary stalk and absence of normal posterior pituitary bright spot on T1 images
Hypothalamic-chiasmatic glioma	Median age of presentation 5-9 years	Vision loss, hydrocephalous, and hypothalamic dysfunction	Lobulated suprasellar masses, hypo- to iso-intense to grey matter on T1W and hyperintense on T2W images Intense enhancement following contrast administration. Can be seen in association with NF1
Sellar and parasellar tuberculosis	Commonly associated with tuberculous meningitis and present as granulomatous hypophysitis	Diabetes insipidus, hypopituitarism or hyperprolactinaemia due to pituitary stalk involvement	Nodular enhancement and thickening of pituitary stalk along with parenchymal tuberculomas and basal exudates
Rathke cleft cyst	Seen in children aged <9 years of age	Usually asymptomatic when small, larger lesions present with headache, visual symptoms and pituitary dysfunction	Usually intrasellar, T1 signal intensity depends on cyst contents, with occasional pseudo-enhancement of cyst walls
Tuber cinereum hamartoma	Most patients aged ≤20 years, more common in boys	Gelastic seizures and precocious puberty	Pedunculated or sessile lesion in region of tuber cinereum, iso-intense to grey matter on all sequences with no contrast enhancement and stable interval size
Langerhans cell histiocytosis	Peak incidence between age 1 and 4 years	Diabetes insipidus	Thickening of pituitary stalk with absence of posterior pituitary bright spot. Additional findings like "punched out" lytic calvarial lesions are specific
Dermoid cyst			Extra-axial midline lesions with MR signal characteristics dependent on the amount of fat content. Usually T1 and T2 hyperintense. Fat- saturated sequences show signal drop of fatty elements. Lack of enhancement differentiates them from teratomas
Epidermoid cyst			Extra-axial off-midline lesions with MR signal intensity similar to CSF on conventional sequences and partial suppression on FLAIR. Restricted diffusion seen on DWI
Metastasis			Imaging features of metastatic disease depend on the underlying pathologic condition and include focal sellar/parasellar lesions, multiple nodular lesions, or nodular leptomeningeal enhancement
Vascular malformations			Usually T2 hyperintense with hypointense rim and SWI sequences show blooming due to recurrent haemorrhages. High-flow vascular lesions show T1 and T2 hypointense flow voids

Abbreviations: CSF = cerebrospinal fluid; CT = computed tomography; DWI = diffusion-weighted imaging; FLAIR = fluid attenuation inversion recovery; MR = magnetic resonance; NF1 = neurofibromatosis type 1; SWI = susceptibility weighted imaging.

C-1676.
12. Papadopoulou E, Chourmouzi D, Drevelegas A. Pediatric sellar: suprasellar tumors. J Pediatr Neuroradiol. 2016;5:82-8.
13. Demaerel P, Van Gool S. Paediatric neuroradiological aspects of Langerhans cell histiocytosis. Neuroradiology. 2008;50:85-92.
14. Rao VJ, James RA, Mitra D. Imaging characteristics of common suprasellar lesions with emphasis on MRI findings. Clin Radiol. 2008;63:939-47.